DEVELOPMENT OF A REPRODUCIBLE AND OPTIMIZED PROTOCOL FOR FREEFORM REVERSIBLE EMBEDDING OF SUSPENDED HYDROGELS

By

OREN JACOB MERHAV

A thesis submitted to the

School of Graduate Studies

Rutgers, The State University of New Jersey

In partial fulfillment of the requirements

For the degree of

Master of Science

Graduate Program in Biomedical Engineering

Written under the direction of

Joseph Freeman

And approved by

_____

_____

_____

New Brunswick, New Jersey

October, 2020

ABSTRACT OF THE THESIS

DEVELOPMENT OF A REPRODUCIBLE AND OPTIMIZED PROTOCOL FOR FREEFORM REVERSIBLE EMBEDDING OF SUSPENDED HYDROGELS

by OREN JACOB MERHAV

Thesis Director:

Joseph Freeman

Organ failure occurs when a bodily system is unable to perform tasks that are necessary for survival, and they can be caused by any significant change to internal body conditions, ranging from chronic diseases to sudden injuries. Long term or irreversible organ failure is most effectively treated with the transplantation of a donated replacement organ as a substitute for the diseased system. The number of patients who require an organ transplant significantly outnumbers available replacements both in the US and worldwide, resulting in many patients dying while on transplant waiting lists. Because organ donations cannot keep up with organ failure prevalence, there exists a need for other avenues of obtaining functional replacements.

3D biofabrication technologies have grown significantly in recent years and show promise as powerful tools in the creation of customizable and biocompatible organ

components and even entire organ structures. However, materials that provide the ideal bioactivity necessary for development of fully functional artificial organs are rarely usable in conventional 3D biofabrication methods due to their incompatibility with high temperatures and inability to maintain their configuration after their extrusion. Recent advancements in a 3D biofabrication technology known as freeform reversible embedding of suspended hydrogels (FRESH), which uses a gelatin microbead support bath to maintain structural integrity, may provide an avenue for using these materials in more versatile ways, but published literature pertaining to this technique is lacking in detail in both material and process. Published material pertaining to FRESH printing also lacks description of how variations in processing steps and material properties affect experimental results, only reporting the specific steps that led to significant results. These information gaps make it difficult for new researchers to recreate and build upon what has already been developed. In order for FRESH printing to progress to the point where it is usable in clinics for creating artificial transplant organs, it is necessary for a full understanding of the technology and its protocols to be accessible.

In this thesis, the beginnings of a detailed FRESH printing protocol are established. It is determined that low blend time in the creation of the gelatin slurry used in FRESH results in a nonuniform support bath that is unusable in printing. This study also produced a protocol for creating a collagen-based bioink using customizable materials and found that existing protocols for FRESH printing using collagen inks may not be broadly effective. Lab closures cause by the COVID-19 pandemic prevented further analysis and protocol building, but a foundation has been laid for an accessible understanding of FRESH printing technologies.

Acknowledgements

First, I would like to thank my research advisor, Dr. Joachim Kohn, for guiding me in the right direction when I needed it most. He has been an excellent mentor, who I greatly admire and respect. I would also like to thank everyone in Dr. Kohn's lab who has helped me throughout my research and provided outside perspectives when tackling difficult roadblocks. The employees of the New Jersey Center for Biomaterials have also been invaluable as resources for support, guidance, and knowledge. I must also thank Dr. Joseph Freeman for taking over as my thesis director on short notice during D. Kohn's absence.

Lastly, I would like to thank my friends and family who have supported me every step of the way and encouraged me to pursue my goals. I am very grateful to all of you for being a part of my academic journey and for helping me achieve so much more than I could have alone.

Table of Contents

ABSTRACT OF THE THESIS ..... *ii*

Acknowledgements ..... *iv*

Table of Contents ..... *v*

Table of Figures ..... *vi*

Introduction *1*

Literature Review *4*

2.1 Organ Failure and Treatment **4**

2.2 Decellularized Organs for Transplant **6**

2.3 3D Biofabrication **8**

2.3.1 Fused Deposition Modeling **8**

2.3.2 Light-Based Biofabrication **9**

2.3.3 Inkjet Printing and 3D Fiber Deposition **9**

2.4 FRESH Printing **10**

2.5 Collagen Bioink **14**

Methods and Materials *16*

3.1 Gelatin Slurry Preparation **16**

3.2 Collagen Extraction **16**

3.3 Collagen Ink Preparation **17**

3.4 Print Testing **18**

Results *19*

4.1 Gelatin Slurry Reproduction **19**

4.2 Collagen Ink Visualization **20**

4.4 Print Tests **21**

4.5 Collagen Crosslinking **21**

Discussion & Conclusions *22*

Future Work *24*

References: *28*

Table of Figures

FIGURE 1. EVERY YEAR, THE GAP BETWEEN THE NUMBER OF KIDNEY TRANSPLANT WAITLIST ADDITIONS AND THE NUMBER OF KIDNEY TRANSPLANT OPERATIONS PERFORMED GROWS [1]. 4
FIGURE 2. PATIENTS WITH END-STAGE RENAL DISEASE EXPERIENCE MUCH LOWER LONG-TERM SURVIVAL RATES WHEN TREATED WITH HEMODIALYSIS THAN WITH A LIVING-DONOR TRANSPLANT [28]. THE DATA REPORTED HERE HAVE BEEN SUPPLIED BY THE UNITED STATES RENAL DATA SYSTEM (USRDS). THE INTERPRETATION AND REPORTING OF THESE DATA ARE THE RESPONSIBILITY OF THE AUTHOR AND IN NO WAY SHOULD BE SEEN AS AN OFFICIAL POLICY OR INTERPRETATION OF THE U.S. GOVERNMENT. 5
FIGURE 3. THE NON-COVALENT BONDS ALLOW THE EXTRUSION OF THE INKS INTO SUPPORT GELS TO DIRECTLY WRITE STRUCTURES CONTINUOUSLY IN 3D SPACE. THIS MATERIAL SYSTEM SUPPORTS THE PATTERNING OF MULTIPLE INKS, CELLS, AND VOID SPACES [56]. 10
FIGURE 4. **(A)** A MODEL OF A HUMAN FEMUR IS FRESH PRINTED IN ALGINATE, AND AFTER REMOVAL FROM THE SUPPORT BATH, IT IS EASILY HANDLED. **(B)** AN EXAMPLE OF THE ARTERIAL TREE PRINTED IN ALGINATE (BLACK) AND EMBEDDED IN THE GELATIN SLURRY SUPPORT BATH. **(C)** A DARK-FIELD IMAGE OF THE 3D PRINTED EMBRYONIC CHICK HEART WITH INTERNAL STRUCTURE VISIBLE THROUGH THE TRANSLUCENT HEART WALL. **(D)** AN EXAMPLE OF 7 IDENTICAL 3D PRINTED BIFURCATED TUBES AND 1 FEMUR USING COLLAGEN INK [20]. 12
FIGURE 5. (**A**) FRESH V1.0 AND (**B**) V2.0, SHOWING THE DECREASE IN SIZE AND POLYDISPERSITY. (**C**) HISTOGRAM OF FERET DIAMETER DISTRIBUTION FOR GELATIN MICROPARTICLES IN FRESH V1.0 (BLUE) AND V2.0 (RED). (**D**) SINGLE FILAMENTS OF COLLAGEN SHOWING THE VARIABILITY OF THE SMALLEST DIAMETER (~250 MM) THAT CAN BE PRINTED USING FRESH V1.0 (TOP) COMPARED TO RELATIVELY SMOOTH FILAMENTS 20 TO 200 MM IN DIAMETER USING FRESH V2.0 (BOTTOM). 13
FIGURE 6. (**A**) SCHEMATIC OF DUAL-MATERIAL FRESH PRINTING USING A COLLAGEN INK AND A HIGH-CONCENTRATION CELL INK. (**B**) VENTRICLE MODEL WITH A CENTRAL SECTION OF CARDIAC CELLS (PINK), INTERNAL AND EXTERNAL COLLAGEN SHELLS (GREEN), AND A COLLAGEN-ONLY SECTION (YELLOW). (**C**) MICROGRAPH OF FRESH-PRINTED VENTRICLE. (**D**) MRI-DERIVED 3D HUMAN HEART SCALED TO NEONATAL SIZE. (**E**) FRESH-PRINTED COLLAGEN HEART [21]. 14
FIGURE 7. GELATIN SLURRY BLENDED FOR (**A**) 60 SECONDS EXHIBITS LARGE CHUNKS OF GELATIN, WHILE SLURRY BLENDED FOR (**B**) 120 SECONDS IS MORE HOMOGENEOUS AND SMOOTH, INDICATING THE PRESENCE OF MICROBEADS RATHER THAN GELATIN CHUNKS. 19
FIGURE 8. (**A**) AT THE START OF THE PRINT, EXTRUDED LINES ARE THIN, AND THEIR BORDERS ARE CLEAR. (**B**) AFTER 6 MINUTES OF CONTINUOUS PRINTING, THE LINES APPEAR MORE BLURRED OR “FUZZY.” 20
FIGURE 9. PRINTED MATERIAL IS SUPPORTED ABOVE THE BOTTOM OF THE SLURRY CONTAINER. 21

Chapter 1

Introduction

According to the Organ Procurement and Transplantation Network, there were 121,696 patients on the United States organ transplant waiting list as of June 17, 2020. However, throughout the entirety of 2019, there were only 39,719 transplant procedures, and a new patient is added to the national transplant waiting list every nine minutes [1]. Because of the large gap between the number of donors and those in need of donation, the wait time to receive an organ can extend up to several years. In the meantime, approximately 8,000 Americans die every year while on the transplant waitlist. Many more are saddled with high medical costs and extremely poor quality of life, as is the case with kidney failure patients requiring hemodialysis [2, 3].

With live organ donors unable to meet the ever-increasing demand for replacement organs, tissue engineers have long sought to supplement the organ supply with functional, artificially grown replicas, as well as fabricated tissue scaffolds that treat the cause of organ failure and avoid the need for a transplant. Although some simpler tissues – those without much structural detail and cellular diversity – have been successfully created in the lab setting, limited complexity stands as a significant obstacle in the path to clinical implementation [4, 5]. In recent years, 3D printing techniques have shown success in creating the necessary complexity, allowing for more intricate structure [6-9], and material customization [10, 11], as well as improved mimicry of biological mechanical properties and heterogeneity [9].

The majority of 3D printing biofabrication techniques involve fused deposition modeling (FDM), 3D fiber deposition modeling (3DF), stereolithography (SLA), digital

light processing (DLP), selective light sintering (SLS), and inkjet printing [12]. However, each of these techniques face difficulties in printing live cells and soft biomaterials. FDM involves high heat that kills cells and denatures proteins, and SLA and DLP methods require the use of photo-curable polymers, which are toxic to cells and unusable for organ or graft printing [13]. Inkjet printing and 3DF methodologies have shown successes in printing biomaterials that support cells, extracellular matrix (ECM) for example, but they are often too low in viscosity to create complex 3D structures. Unsupported filaments droop, and base edges spread, thus limiting inkjet printing to 2D designs or non-biocompatible filaments [13-15]. While 3D biofabrication is useful in developing and prototyping medical devices, such as microphysiological systems [16], and basic structures, such as perfusable networks [17-19], the mechanical properties of the required materials create challenges in organ and graft printing.

One way to support materials with poor structural integrity is with the use of a sacrificial material, which holds printed filaments in place during an intermediate period of chemical cross-linking before ultimately being removed entirely. Feinberg *et al.* has demonstrated particular success in tackling this problem in the development of techniques for freeform reversible embedding of suspended hydrogels (FRESH). FRESH printing involves the use of gelatin microparticles as a support bath for low-viscosity bioinks. The bath allows an extrusion needle to pass through easily, while holding deposited material in place and refilling gaps created by the needle. This technique has been used to create 3D reconstructions of vasculature and small bones [20], as well as a high-resolution model of a human heart [21], using soft, collagen-based bioinks capable of supporting living cells.

While their successes are impressive, their publications leave out crucial details that are necessary for the reproduction of their methods, complicating the efforts of outside scientists who hope to contribute to novel FRESH techniques. Additionally, they have reported very little regarding the relationships between various processing parameters and aspects of their final print, instead focusing only on the parameters used in their successful prints.

The goal of this study is to examine the effects of variations in FRESH printing parameters used by Hinton *et al.* on a selection of printing metrics. This will aid in future efforts to improve and expand FRESH printing methods. Specifically, this study aimed to investigate changes in gelatin bloom and concentration, $CaCl_2$ concentration, and blend time used in the creation of the thermoreversible gelatin bath. The effects of these changes were to be analyzed based on the properties of the bath, including its ability to self-heal, bath homogeneity, and microparticle size, as well as printing metrics, including maintained resolution similarity between printed structures and STL file parameters. However, due to lab closures, the investigation was limited to the effects of blend time on the ability of the bath to self-heal and its homogeneity.

Chapter 2

Literature Review

2.1 Organ Failure and Treatment

Organ failure describes the complete loss of biological function in a system that is essential for an organism's survival. It has a variety of causes, ranging from inadequate treatment of chronic disease [22] to sudden changes in internal body conditions, such as heart attacks, injuries, or sepsis [23, 24], and treatments vary depending on the acuity and location of the dysfunction. Because long term therapies often significantly reduce the patient's quality of life and are rarely permanent solutions, organ transplantation is considered the optimal treatment for irreversible organ failure [25], but the availability of organs for transplant falls far short of their demand. For example, the waitlist for kidney transplant makes up over 80% of the entire organ transplant waitlist [1], and waitlist registrations outweigh transplant operations more every year, as shown in Figure 1.

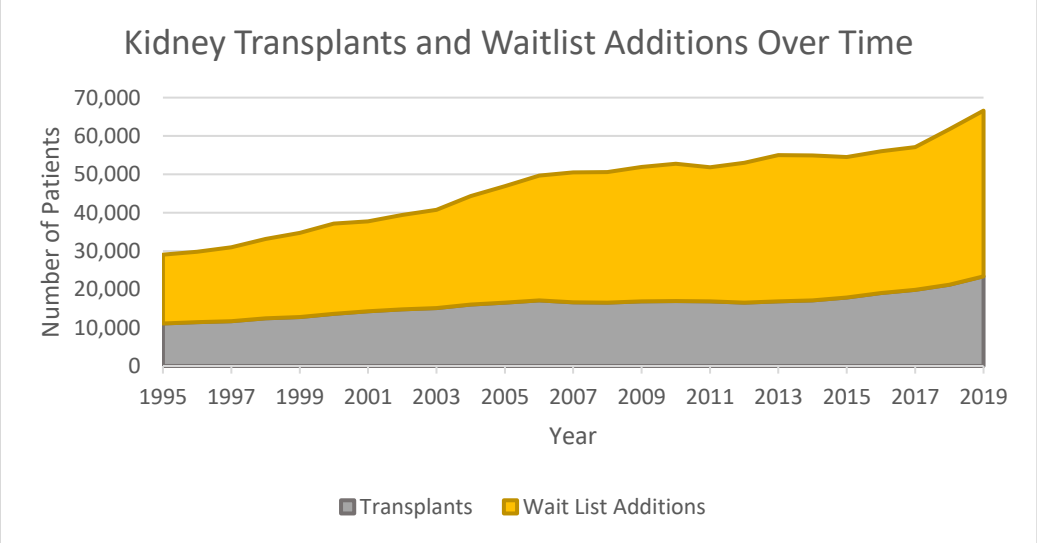

Figure 1. Every year, the gap between the number of kidney transplant waitlist additions and the number of kidney transplant operations performed grows [1].

Renal replacement is most often required by patients with end-stage chronic kidney disease (CKD), who face two treatment options: kidney replacement or hemodialysis, in which the patient's blood is filtered externally by a system of tubes. Hemodialysis can extend a patients' lives without proper renal function, but they are required to frequently spend long periods of time in dialysis centers [2, 3]. This process is also very expensive and not available in many communities without adequate financial means [26, 27], and even those who do access hemodialysis treatment experience far lower survival rates than those who receive a transplant, as shown in Figure 2.

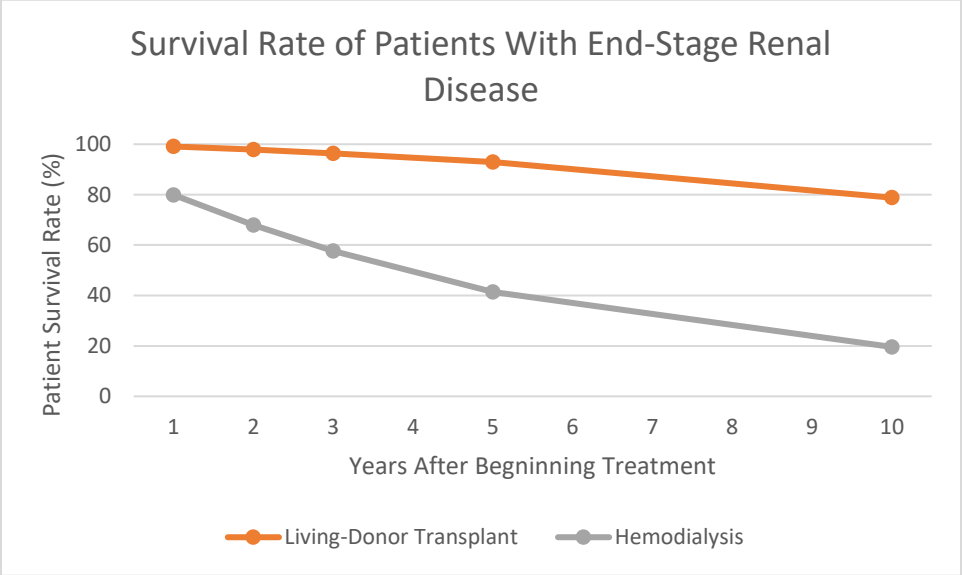

Figure 2. Patients with end-stage renal disease experience much lower long-term survival rates when treated with hemodialysis than with a living-donor transplant [28]. The data reported here have been supplied by the United States Renal Data System (USRDS). The interpretation and reporting of these data are the responsibility of the author and in no way should be seen as an official policy or interpretation of the U.S. government.

Despite its shortcomings, hemodialysis is still widely administered due to the significant and increasing gap between kidney supply and demand. With the highest

demand for transplantation treatments, kidney failure garners the most attention, but other organs diseases face similar problems. Transplantation is also the most effective treatment for end-stage heart failure [29], subacute liver failure [30], and lung disease [31], among other diagnoses. Nearly all organ transplants statistics are outweighed by wait list registrations with proportions similar to that of kidney transplants [1].

2.2 Decellularized Organs for Transplant

The gap between organ supply and demand can be filled either by obtaining more organs from existing sources (i.e. organ donors) or by developing alternate sources. While creating a mass influx of donor registrations may require feats of public health communication and education, the latter route is more easily charted by scientists and tissue engineers.

Organ decellularization may allow for expansion of the organ donor pool beyond living humans and fresh, formerly healthy cadavers to terminally ill patients and even animals. This involves the removal of cells from a donor organ or tissue samples, often using a detergent or enzyme, and the subsequent introduction, perfusion, and growth of host cells into the remaining tissue structure. Such techniques have already been successfully employed in the development of ECM grafts with already-made vascular structures and have shown promise in the area of whole organ transplants [32-35], but they are a long way from clinical use due to several challenges.

First, decellularized organs are still donor-derived products that are not immune to the donor shortages already facing organ transplantation. While the removal of diseased cells may allow for some ill patients and their cadavers to donate, recent findings suggest that some diseases create structural changes in ECM structure, extending illness to

reintroduced cells [36]. Organs obtained from animals are currently utilized for the regeneration of organ components and tissue segments, but the transplantation of entire organs into humans may face problems in structural compatibility [37]. Thus, the donor pool expansion, while helpful, may still fall short of organ demand.

Decellularized organs are also prone to triggering an immune response within the host, as even a small amount of donor DNA left intact or leftover enzymes from the decellularization process can cause an adverse host response [37-39]. While the complete decellularization of organ components and ECM samples is possible with relatively simple diffusion-based methods [40], the perfusion-based decellularization techniques required for larger, whole organs are more complex and prone to error [41].

Lastly, many successes in decellularized organ transplantation have been achieved in small animals, such as rats and mice, and only for short time periods [42]. Meanwhile, the extension of this technology to larger organs and longer time frames necessary for this application faces obstacles in the scaling of recellularization techniques. All organs contain within them a diverse cell population with specific proportions of different specialized cells and each type of cell specifically placed, and the ability to coculture and place such necessary diversity has not yet been demonstrated. For instance, a major advantage of decellularized organs is their intact vasculature, but the vasculature is only useful when fully seeded with endothelial cells, and this has not been successfully accomplished with long term cell survival [43].

2.3 3D Biofabrication

Another potential alternate source of organs for transplantation lies in the ground-up construction of organ structures that are either built for cell seeding or created with cells incorporated within the structure itself. This cutting-edge field involving artificial methods of organ growth and repair is known as biofabrication, and its sub-field of 3D biofabrication employs the use of additive manufacturing techniques to meet this goal. By starting with raw materials, organs produced though 3D biofabrication would avoid supply limitations created by donor shortages and do not require any sort of complex decellularization process. Additionally, as discussed later on, certain 3D biofabrication techniques allow for the specific placement of living cells during organ construction.

2.3.1 Fused Deposition Modeling

Partly responsible for recent growth in 3D biofabrication is the expiration of patents and lowered equipment costs involved in FDM [13, 44], possibly the most well-known of the additive manufacturing technologies. This process involves rollers pushing a polymer filament through a heating chamber, where it is melted and fed through a nozzle. As the melted polymer exits the nozzle, it is deposited onto a stage, and the nozzle and stage move to place material in specified patterns. The material cools and hardens, and subsequent layers are deposited on top [12, 45, 46]. FDM is a powerful tool for rapid prototyping and even for the construction of some cell scaffolds, but its reliance on high temperatures precludes the use of biological factors and thermolabile natural biomaterials that influence cell growth and behavior.

2.3.2 Light-Based Biofabrication

Other additive manufacturing techniques utilize lasers that trace each layer's design onto powdered or liquid material. In conventional SLS techniques, a thin layer of polymer grains is spread across a stage. As the polymer absorbs the laser light, it heats and fuses. Then a new layer of powder is added, and the process repeats [47]. As with FDM, SLS's use of heat limits its use in biofabrication. In surface SLS, the light is absorbed by carbon microparticles distributed on the surface of the powder grains. This melts only the surfaces of the grains, allowing for the release of bioactive compounds trapped inside, which bind particles together [48]. However, due to a lack of research regarding the use of these bioactive compounds and the biocompatibility of carbon microparticles, surface SLS is far from mature enough to be used in biofabrication [49]. SLA and DLP employ techniques similar to SLS, using a liquid photosensitive polymer resin in place of powder. These methods also face obstacles in biofabrication applications due to the toxicity of photopolymers [13].

2.3.3 Inkjet Printing and 3D Fiber Deposition

As discussed earlier, many biofactors and cell-supporting materials that are ideal for cell scaffold construction become damaged at the high heat required to melt them into a printed formation. Inkjet bioprinting and 3DF are techniques designed for use with soft materials that can be printed at room temperature, and they are compatible with bioink formulations of proteins, including collagen [50-52], fibrin [53, 54], and gelatin [9]. Their use of nonsolid printing materials also allows for functionality in printing formulations with cells incorporated into the bioink [9, 52, 55]. Inkjet bioprinting operates in a similar fashion to traditional inkjet printing. As a printhead moves across the stage, bioink is

dispensed from thousands of nozzles in a specified pattern. High resolution and material customization make inkjet printing a valuable tool in 2D constructions, but because it requires viscosities low enough to pass through the small printhead nozzles, inkjet bioinks struggle to maintain 3D structures [12, 13].

3DF is more similar to FDM, with the key difference being the low temperatures used in printing. In 3DF, bioink is loaded into a cartridge or syringe and extruded with positive pressure. As with inkjet printing, the use of bioinks in place of melted filaments creates challenges in the construction of 3D designs. However, this hurdle can be overcome by extruding the bioink into a support material that suspends fibers and is later removed (Figure 3) [20, 56-58]. Thus, the ability to print complex 3D structures using soft biological materials makes 3DF the most promising additive manufacturing technique for use in biofabrication.

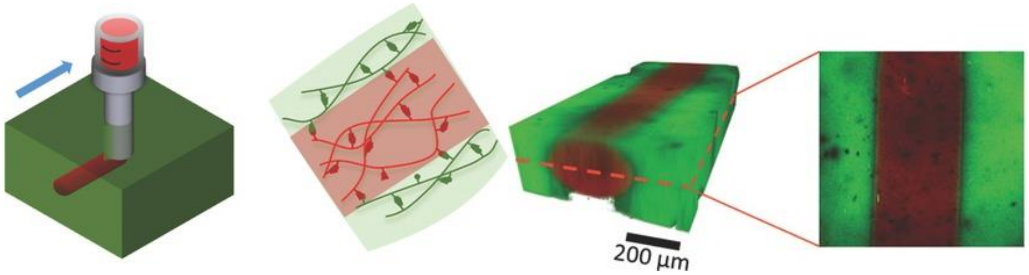

Figure 3. The non-covalent bonds allow the extrusion of the inks into support gels to directly write structures continuously in 3D space. This material system supports the patterning of multiple inks, cells, and void spaces [56].

2.4 FRESH Printing

Developed by the Regenerative Biomaterials & Therapeutics Group at Carnegie Mellon University, FRESH printing methods incorporate a thermoreversible support bath into 3DF techniques.

> "The support bath is composed of gelatin microparticles that act like a Bingham plastic during the print process, behaving as a rigid body at low shear stresses but flowing as a viscous fluid at higher shear stresses. This means that, as a needle-like nozzle moves through the bath, there is little mechanical resistance, yet the hydrogel being extruded out of the nozzle and deposited within the bath is held in place. Thus, soft materials that would collapse if printed in air are easily maintained in the intended 3D geometry" [20].

Depending on the bioink components used, the support bath is supplemented with a cross-linking agent. Once the ink is fully crosslinked into a solid structure, the ink and bath are incubated at 37°C. At this temperature, the gelatin slurry microparticles dissolve, and the bath melts away allowing for the 3D printed structure to be easily removed [20].

Hinton *et al.* have demonstrated various successes with FRESH printing technologies in recent years. With the introduction of FRESH in 2015, they showcased its capabilities by creating models of a bone, an arterial tree, and an embryonic chicken heart from alginate, as well as a femur model and bifurcated tubes from collagen ink (Figure 4) [20]. With what they later named "FRESH 1.0," they were able to create microbeads as small as 65 μm in average diameter. However, this process involves imperfect mechanical blending of gelatin to form beads, resulting in significant variation in bead size and irregular bead shapes (Figure 5A,C). Gelatin slurries made with this process supported the reliable printing of fibers ~250 μm in diameter at the smallest (Figure 5D) [21].

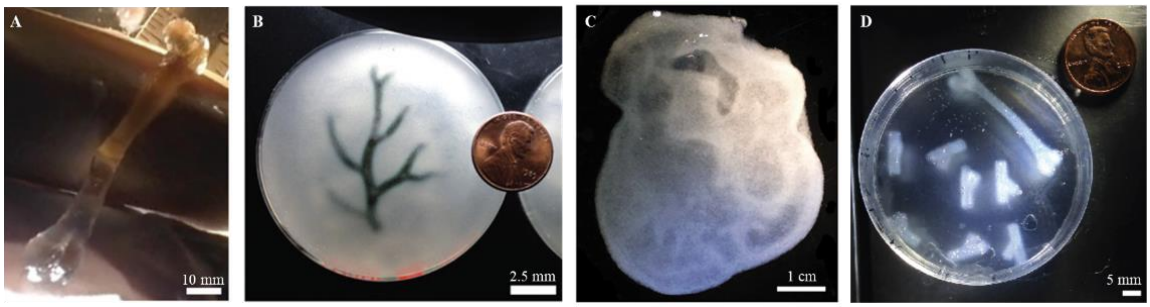

Figure 4. **(A)** A model of a human femur is FRESH printed in alginate, and after removal from the support bath, it is easily handled. **(B)** An example of the arterial tree printed in alginate (black) and embedded in the gelatin slurry support bath. **(C)** A dark-field image of the 3D printed embryonic chick heart with internal structure visible through the translucent heart wall. **(D)** An example of 7 identical 3D printed bifurcated tubes and 1 femur using collagen ink [20].

Later, with the development their FRESH 2.0 methods in 2019, Lee *et al.* successfully printed human heart components loaded with cardiomyocytes and a neonatal human heart model using collagen ink. FRESH 2.0 involves a complex coacervation method rather than mechanical blending to produce an improved support bath. With this method, gelatin microparticles were created with much more spherical shapes, less variation in size, and a consistently smaller average diameter of 25 μm (Figure 5B,C). The FRESH 2.0 support bath allowed them to achieve fiber diameters as low as 20 μm (Figure 5D) and structures as large as 55 mm in height (Figure 6) [21]. No exact correlations between the physical microbead properties and the fiber resolutions they support are reported in these studies, but it appears that smaller beads are able to support smaller fiber extrusions and that reduced variation in bead size and shape improve reliability and consistency when printing fibers with comparable diameters to the beads themselves.

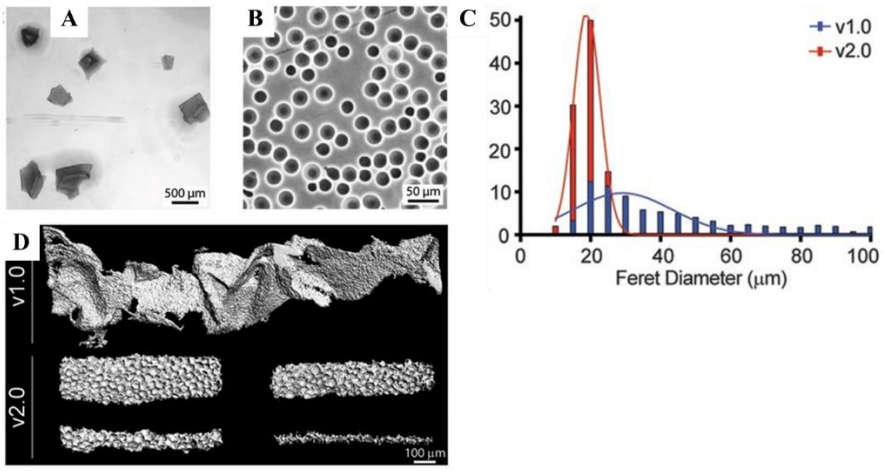

Figure 5. (**A**) FRESH v1.0 and (**B**) v2.0, showing the decrease in size and polydispersity. (**C**) Histogram of Feret diameter distribution for gelatin microparticles in FRESH v1.0 (blue) and v2.0 (red). (**D**) Single filaments of collagen showing the variability of the smallest diameter (~250 µm) that can be printed using FRESH v1.0 (top) compared to relatively smooth filaments 20 to 200 µm in diameter using FRESH v2.0 (bottom).

It is expected that replicating the methods used to create FRESH 1.0 by Hinton *et al.*, keeping as many parameters consistent with theirs as possible, will produce a gelatin bath capable of reliable support and cross-linking of collagen filaments as small as 250 µm. With such major gaps in their methods, as discussed in Chapter 1, it is impossible to determine how closely the methods used in this study align with theirs. Because of this, some variation in gelatin bath and collagen bioink quality is expected. For the print test performed in this study (Chapter 3.4), collagen filaments are extruded through a 21 G needle, which have a nominal inner diameter of close to 500 µm, to account for this.

While the Feinberg lab's proof of concept shows great promise in one day bringing fully 3D printed organs to clinical use, FRESH printing techniques have yet to be demonstrated outside of the Feinberg lab. This difficulty in method reproduction may be caused in part by insufficient explanation of their methods in published literature and a

gap in the understanding of how variations in FRESH processes affect the mechanical and biological properties of printed grafts and organs. We believe that the development of a detailed FRESH printing protocol, starting with the simpler FRESH 1.0 process, and a comprehensive comparison of processing parameters will allow for the improved collaboration and innovation required to bring biofabrication technologies past the early development stage.

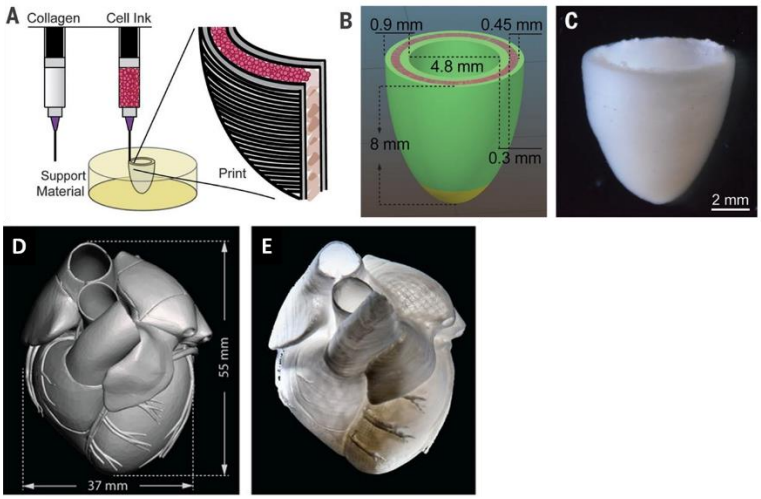

Figure 6. (**A**) Schematic of dual-material FRESH printing using a collagen ink and a high-concentration cell ink. (**B**) Ventricle model with a central section of cardiac cells (pink), internal and external collagen shells (green), and a collagen-only section (yellow). (**C**) Micrograph of FRESH-printed ventricle. (**D**) MRI-derived 3D human heart scaled to neonatal size. (**E**) FRESH-printed collagen heart [21].

2.5 Collagen Bioink

Collagen was selected as a base for this study's bioink because of its utility and popularity in the tissue engineering space. Comprising around 20-30% of all vertebrate protein [59], collagen is readily available and exhibits very high biocompatibility and low

antigenicity [60]. 3D printed collagen-based cell scaffolds have been applied toward bone regeneration [50] and cartilage growth [51], and toward mimicking the physical properties of brain tissue [61, 62], menisci [63], and other tissue types.

Collagen bioinks are often difficult to use in 3D printing techniques because of their low viscosity and lack of structural integrity [64]. Collagen has been shown to cross-link effectively into a gel in the presence of calcium chloride, but only when maintained at a pH of 7.4 and a temperature of 37°C for at least 1 hour [21]. If left unsupported during this time, the collagen will lose the geometry it was printed in. However, recent technological advances in embedded hydrogel printing greatly expand the scope of applications for such materials.

Chapter 3

Methods and Materials

3.1 Gelatin Slurry Preparation

Three batches of gel slurry were prepared by mixing 4.5% (w/v) gelatin from porcine skin (300g bloom, Type A, Thermo Fisher Scientific) into 150 mL of 11 mM $CaCl_2$ (Amresco). The solution was heated in a 1000 W microwave for 30 seconds to aid in the dissolution and then gelled at 4°C overnight. After 18 hours at 4°C, the gel was blended at pulse speed (Osterizer Classic) together with 350 mL of 11 mM $CaCl_2$ solution chilled to 4°C. In each batch, half of the slurry was removed after 60 seconds of blend time, and the remainder was blended for an additional 60 seconds for a total of 120 seconds of blend time. The slurry was moved to conical tubes and centrifuged at 3750 RPM for 2 minutes. Bubbles were then removed from each tube using a pipette, and the tubes were again centrifuged at 3750 RPM for 2 minutes. All tubes were stored at 4°C overnight.

3.2 Collagen Extraction

The collagen ink used in this study was made using collagen extracted from rat tails. First, the rat tails were soaked in 70% ethanol for 20 minutes. Each tail was then held under ethanol using a hemostat, and a scalpel was used to make a shallow incision from end to end. The skin was then peeled away to expose the tendons. Each tendon was then pulled out of its sheath in the direction of the tail end using forceps. As each tendon was extracted, it was stored in 70% ethanol. After the extraction, the tendons were patted

dry and added to a 0.1% acetic acid solution at 150 mL/gram of tendon. The collagen was let to solubilize for 48 hours at 4°C.

After the solubilization period, the collagen solution was centrifuged at 9000 RPM for 90 minutes to remove any unsolubilized collagen, blood, muscle tissue, and other impurities. The clear supernatant was collected and any pellets were removed. The collected supernatant solution was frozen at -80°C for 30 minutes and lyophilized for 48 hours.

3.3 Collagen Ink Preparation

We created our own collagen bioink instead of using a commercially available option because future studies that employ FRESH printing techniques may require variations in ink composition that are not easily purchased. The collagen bioink used in this study's 3D printing experiments was created using methods described by Hinton *et al.* [20], with manually extracted rat tail collagen substituted for the purchased rat tail collagen used in their study. The extraction is described in section 3.2. 9.2 mg/mL collagen was stirred together with 0.02 N acetic acid solution. Large impurities were identified and removed manually. The ink was then stored at 4°C overnight.

Because the printer used in 3D printing experiments does not apply a large amount of force in bioink extrusion, any small undissolved impurity larger than the needle's inner diameter can cause blockages that prevent effective printing. Therefore, the ink was filtered before use. The high viscosity of the ink required significant pressure to be used in the filtration process. Initially, the ink was filtered by being loaded into a syringe and manually pushed through a 22 G needle, as this is the size used in printing experiments. When a blockage was encountered, the needle was removed and the

impurity causing the blockage was manually extracted from the solution. However, the orientation of the impurity particles sometimes allowed them to pass through the needle, only to cause a blockage later in printing. This process also resulted in significant losses of material. This method of filtration was determined to be far too time-consuming and ineffective for practical use.

Effective filtration was accomplished using a 300 μm mesh filter attached to a syringe using a Luer-Lok attachment. The collagen bioink was manually pushed through the filter mesh. After filtration, rhodamine was mixed into the bioink at a concentration of 100 μg/mL of bioink for improved visibility.

3.4 Print Testing

All prints were executed using a r3bEL Mini Bioprinter from SE3D. A syringe with a 22 G needle was filled with collagen bioink and loaded onto the printer. The ink was deposited through a 21 G needle into gelatin slurry that was blended for 120 seconds. All 3D designs were modeled using Google Sketchup and converted to STL files using Slic3r.

Chapter 4

Results

4.1 Gelatin Slurry Reproduction

The only experimental processing parameter tested before lab closures was the blend time. From this, we determined that with our procedure, slurry blended for 60 seconds had greatly reduced homogeneity relative to slurry from the same bath blended for 120 seconds (Figure 7).

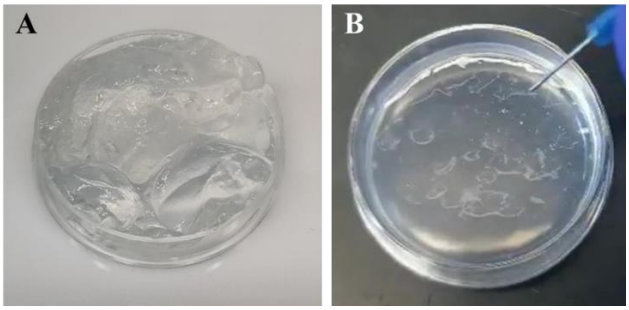

Figure 7. Gelatin slurry blended for (**A**) 60 seconds exhibits large chunks of gelatin, while slurry blended for (**B**) 120 seconds is more homogeneous and smooth, indicating the presence of microbeads rather than gelatin chunks.

The self-healing ability of the slurry blended for 60 seconds was not possible, as running a needle through the slurry caught chunks of gelatin and moved them around rather than passing through. The slurry blended for 120 seconds was successful in self-healing. Supplemental Video S1 shows an 18G needle passing through the slurry with no visible fissure left behind.

Although these results were consistent across all three batches, the consistency of slurry blended for 30 seconds varied significantly. In one batch, the chunks that appeared were small and shifted easily. While the portion of this batch blended for 30 seconds still

showed reduced homogeneity relative to the portion blended for 60 seconds, the difference was much smaller than in the other two batches. In those batches, portions blended for 30 seconds had significantly larger chunks that moved as solid pieces as a needle passed through them.

4.2 Collagen Ink Visualization

Rhodamine dye was mixed into the collagen bioink for the purpose of improved visualization of printed material, as the collagen ink is otherwise clear. During printing, lines of extruded ink appeared to spread and lose definition over time (Figure 8).

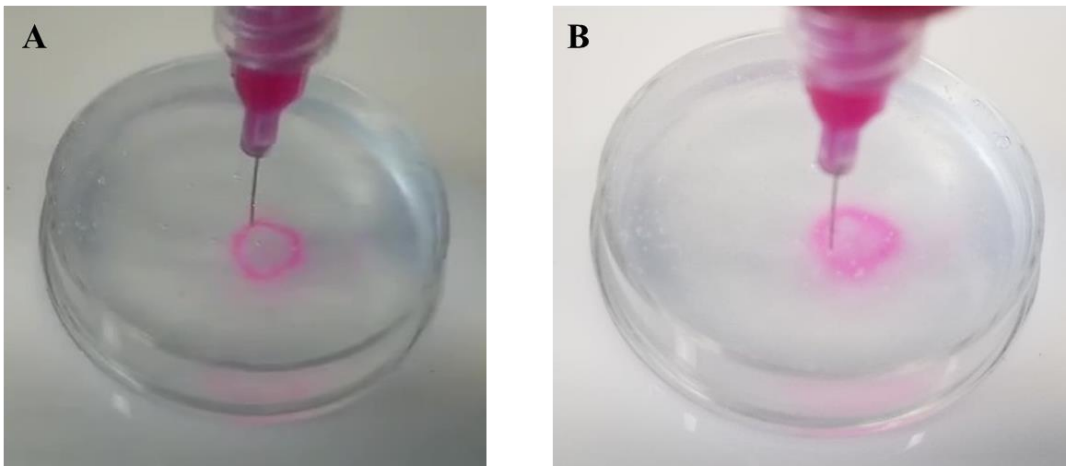

Figure 8. (**A**) At the start of the print, extruded lines are thin, and their borders are clear. (**B**) After 6 minutes of continuous printing, the lines appear more blurred or "fuzzy."

This may suggest that the collagen ink itself is dissolving into the bath and that this bioink is not suitable for FRESH printing. However, this may also be explained by the rhodamine diffusing into the bath away from the collagen and that rhodamine is not a suitable dye for this type of ink. It is also possible that shifts in the bath caused by needle movement caused the ink to spread during printing.

4.4 Print Tests

Prior to printing, 10 mM HEPES was added to the support slurry in order to ensure collagen crosslinking by maintaining a pH of ~7.4 and neutralizing the acetic acid. A small dome shape was successfully printed from collagen ink into slurry blended for 120 seconds. Figure 9 shows the ability of the slurry to hold extruded ink stationary in 3D space during printing.

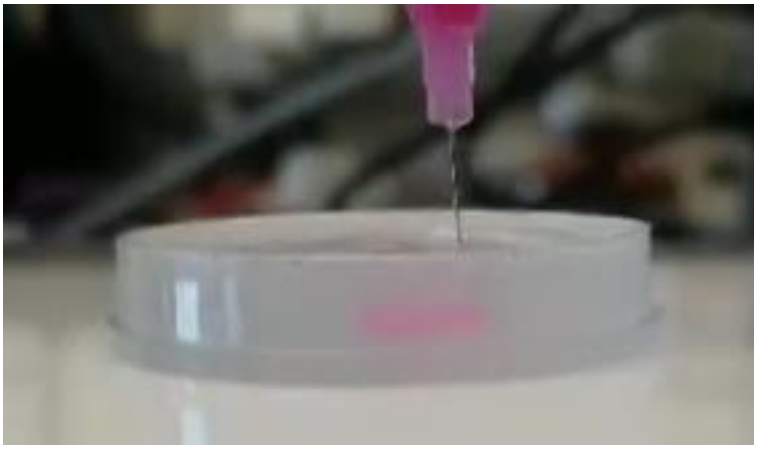

Figure 9. Printed material is supported above the bottom of the slurry container.

4.5 Collagen Crosslinking

The dome print shown in 4.3 was not visible after incubation. As discussed in 4.2, the rhodamine may have diffused away from the printed collagen, making it difficult to see. Otherwise, this may suggest that the collagen bioink did not successfully crosslink after its extrusion and fully dissolved into the surrounding solution during the incubation period.

Chapter 5

Discussion & Conclusions

3D biofabrication is an inherently complicated field, combining the numerous inputs involved in 3D printing with the unforgiving nature and variability of biologically derived materials. Because of this, the establishment of highly detailed working protocols for new biofabrication technologies, like FRESH printing, is vital to the reproduction of results and to the progression of this field. The high sensitivity of biofabrication systems makes it so that even small changes in processing or in material parameters can drastically reduce the utility and effectiveness of such techniques, and the work required to determine optimal parameters is painstaking and difficult. However, those that have completed this work paint an incomplete picture in their publications of what they have determined to be optimal parameters, leaving other groups to redo this work themselves and hindering the advancement of biofabrication methods.

The work in this thesis takes the first step in determining these optimal parameters with the intention of publishing them for use in future studies. The goals were to develop a detailed protocol for reproducible FRESH printing methods and to determine relationships between various processing parameters and printing and material metrics. Through this study, it was established that short blend times used in the preparation of gelatin slurry result in chunks of gelatin that are not suitable for printing, while longer blend times improve homogeneity and do not necessarily negatively affect its ability to support printed material. A protocol for creating a printable bioink from rat tail collagen was also developed, and it was found that published crosslinking techniques used for

collagen bioinks in FRESH printing may not work effectively with a more customized ink.

Due to COVID-19 lab closures, the analysis required for determining further relationships was not possible, and a full working protocol was not fully established. However, the stage has been set for future research to execute these tasks more smoothly. The level of detail provided is designed to help future researchers build on what was learned in this study and avoid having to repeat experiments due to unclear instruction. Because of the work accomplished in this study, future researchers will be better prepared to optimize material and process specifications in the creation of gelatin slurries and collagen-based bioinks.

Chapter 6

Future Work

Due to lab closures stemming from the current coronavirus pandemic, many of the initially intended metrics were not measured, and most planned gel slurry batches were not created. This section details an experimental design that will allow future research to home in on specific processing steps and materials to determine their effects on printability. These steps, materials, and effects can be categorized based on the aspect of FRESH printing they target, including the bath, the ink, and the printing setup.

As discussed previously, the protocols for creating the gelatin bath that is characteristic of FRESH techniques lack details that are vital to their repeatability and reproducibility. Future research aiming to develop a detailed protocol for FRESH printing would benefit from filling in these gaps through experimentation. Gelatin bloom strength, for example, is not mentioned in any published literature relating to FRESH printing. As the bloom strength determines the molecular weight of the gelatin, this may significantly affect the mechanical properties of gelatin microbeads. There is also little known regarding the effects of varied gelatin and calcium chloride concentrations on microbead properties. For example, reducing the gelatin concentration may reduce the likelihood of the formation of chunks in the slurry like those observed in this study, increasing homogeneity without additional blending, which risks forcing the gelatin back into solution, as observed by Hinton *et al.* Reducing the concentration of gelatin may also result in lower bath viscosity, affecting its ability to keep extruded bioink filaments at rest during printing, so multiple metrics must be used to determine how these changes affect the bath. The effects of varying these parameters can be assessed through analyzing the

gelatin baths' ability to self-heal, homogeneity, and viscosity. Determining the relationships between these parameters and the physical characteristics of microbeads may also provide valuable information for the baths' tunable characteristics. Changes in calcium chloride concentration are likely to affect microbead geometry, and an increase may produce more regularly shaped beads. Characteristics like shape, size, and polydispersity can be determined using microscopy techniques. One possible experimental design for testing these parameter variations, including interactions between these parameters, is provided in Table 1.

Once it is understood how variations in gelatin bath protocols affect bath properties, future researchers can determine relationships between these properties and print quality. For example, studies can be designed to determine the relationship between microbead size and achievable print resolution. As discussed in Chapter 2.4, it appears that reduced microbead Feret diameter and polydispersity, together with more spherical bead shapes, allow for the printing of smaller bioink filaments and for improved filament reliability, and so this is the expected result. However, experiments pertaining to these relationships have not been published, and the cause of FRESH 2.0's improved metrics has not been determined with certainty. With an understanding of how processing and materials affect different aspects of FRESH printing and of how these aspects affect print metrics, researchers will have avenues available to them for the creation of tunable characteristics and optimized FRESH methodologies for a wide range of applications.

If future researchers opt to continue using collagen-based bioinks, it would also be beneficial to develop tools for improved visualization, as well as to determine the effects of different crosslinking techniques on printing metrics. This study faced

difficulties in staining and crosslinking extruded bioink, which impeded the analysis of finished prints. Any future analysis of printing metrics may require improved methods of bioink visualization and crosslinking. Improved visualization may be accomplished by using a dye whose molecules are much larger than rhodamine's and will take much longer to diffuse away, such as activated charcoal, allowing the bioink to crosslink and trap the dye inside before it escapes. Alternatively, a dye could be chemically bound to the collagen. This can be accomplished using azo-dyes [65], or with fluorescent labeling [66], but both require additional processing of the collagen bioink that may alter its material and chemical properties. If the collagen crosslinking methods used here are found to be inadequate, EDC-NHS coupling provides a possible alternative, as it has been used to cross-link collagen without damaging fibers [67]. The use of these tools with FRESH printing techniques are worth further experimentation to determine their effectiveness and their effects on collagen ink printability.

Batch Number	Gelatin Bloom Strength (g)	Gelatin Concentration (%w/v)	Calcium Chloride Concentration (mM)	Blend Time (s)
1	100	2.75	11	60
2				120
3				180
4			22	60
5				120
6				180
7		4.5	11	60
8				120
9				180
10			22	60
11				120
12				180
13	300	2.75	11	60
14				120
15				180
16			22	60
17				120
18				180
19		4.5	11	60
20				120
21				180
22			22	60
23				120
24				180

Table 1. A possible experimental design for future researchers looking to analyze gelatin bath properties and their relationships to changes in various processing and material parameters, as well as interactions between these parameters.

References:

1. *2019-2020 Annual Report of the U.S. Organ Procurement and Transplantation Network and the Scientific Registry of Transplant Recipients: Transplant Data*. 2019-2020.
2. Fukuhara, S., et al., *Health-related quality of life among dialysis patients on three continents: the Dialysis Outcomes and Practice Patterns Study.* 2003. **64**(5): p. 1903-1910.
3. Weisbord, S.D., et al., *Symptom burden, quality of life, advance care planning and the potential value of palliative care in severely ill haemodialysis patients.* 2003. **18**(7): p. 1345-1352.
4. Mikos, A.G., et al., *Engineering complex tissues.* Tissue Eng, 2006. **12**(12): p. 3307-39.
5. Atala, A., F.K. Kasper, and A.G. Mikos, *Engineering complex tissues.* Sci Transl Med, 2012. **4**(160): p. 160rv12.
6. Xu, T., et al., *Complex heterogeneous tissue constructs containing multiple cell types prepared by inkjet printing technology.* 2013. **34**(1): p. 130-139.
7. Mironov, V., et al., *Organ printing: tissue spheroids as building blocks.* 2009. **30**(12): p. 2164-2174.
8. Durmus, N.G., S. Tasoglu, and U.J.N.m. Demirci, *Bioprinting: functional droplet networks.* 2013. **12**(6): p. 478-479.
9. Kolesky, D.B., et al., *3D bioprinting of vascularized, heterogeneous cell-laden tissue constructs.* 2014. **26**(19): p. 3124-3130.
10. Murphy, S.V. and A.J.N.b. Atala, *3D bioprinting of tissues and organs.* 2014. **32**(8): p. 773.
11. Jones, N., *Science in three dimensions: the print revolution*. 2012.
12. Kelly, C.N., et al., *Design and structure–function characterization of 3D printed synthetic porous biomaterials for tissue engineering.* 2018. **7**(7): p. 1701095.
13. Gibson, I., D.W. Rosen, and B. Stucker, *Additive manufacturing technologies*. Vol. 17. 2014: Springer.
14. Gao, G., et al., *Bioactive nanoparticles stimulate bone tissue formation in bioprinted three-dimensional scaffold and human mesenchymal stem cells.* 2014. **9**(10): p. 1304-1311.
15. Gao, G., et al., *Inkjet-bioprinted acrylated peptides and PEG hydrogel with human mesenchymal stem cells promote robust bone and cartilage formation with minimal printhead clogging.* 2015. **10**(10): p. 1568-1577.
16. Edington, C.D., et al., *Interconnected microphysiological systems for quantitative biology and pharmacology studies.* 2018. **8**(1): p. 1-18.
17. Grigoryan, B., et al., *Multivascular networks and functional intravascular topologies within biocompatible hydrogels.* 2019. **364**(6439): p. 458-464.
18. Miller, J.S., et al., *Rapid casting of patterned vascular networks for perfusable engineered three-dimensional tissues.* 2012. **11**(9): p. 768-774.
19. Kolesky, D.B., et al., *Three-dimensional bioprinting of thick vascularized tissues.* 2016. **113**(12): p. 3179-3184.

20. Hinton, T.J., et al., *Three-dimensional printing of complex biological structures by freeform reversible embedding of suspended hydrogels.* 2015. **1**(9): p. e1500758.
21. Lee, A., et al., *3D bioprinting of collagen to rebuild components of the human heart.* 2019. **365**(6452): p. 482-487.
22. Levey, A.S. and J.J.T.l. Coresh, *Chronic kidney disease.* 2012. **379**(9811): p. 165-180.
23. Durham, R.M., et al., *Multiple organ failure in trauma patients.* 2003. **55**(4): p. 608-616.
24. Vincent, J.-L., et al., *The SOFA (Sepsis-related Organ Failure Assessment) score to describe organ dysfunction/failure*. 1996, Springer-Verlag.
25. Grinyó, J.M.J.C.S.H.p.i.m., *Why is organ transplantation clinically important?* 2013. **3**(6): p. a014985.
26. Jha, V., et al., *Chronic kidney disease: global dimension and perspectives.* 2013. **382**(9888): p. 260-272.
27. Collins, A.J., et al., *'United States Renal Data System 2011 Annual Data Report: Atlas of chronic kidney disease & end-stage renal disease in the United States.* 2012. **59**(1 Suppl 1): p. A7, e1.
28. *2019 USRDS annual data report: Epidemiology of kidney disease in the United States*. 2019, National Institutes of Health, National Institute of Diabetes and Digestive and Kidney Diseases, Bethesda, MD.
29. Friedrich, E.B. and M.J.H. Böhm, *Management of end stage heart failure.* 2007. **93**(5): p. 626-631.
30. Stravitz, R.T.J.C., *Critical management decisions in patients with acute liver failure.* 2008. **134**(5): p. 1092-1102.
31. De Meester, J., et al., *Listing for lung transplantation: life expectancy and transplant effect, stratified by type of end-stage lung disease, the Eurotransplant experience.* 2001. **20**(5): p. 518-524.
32. Ott, H.C., et al., *Perfusion-decellularized matrix: using nature's platform to engineer a bioartificial heart.* 2008. **14**(2): p. 213-221.
33. Uygun, B.E., et al., *Organ reengineering through development of a transplantable recellularized liver graft using decellularized liver matrix.* 2010. **16**(7): p. 814-820.
34. Petersen, T.H., et al., *Tissue-engineered lungs for in vivo implantation.* 2010. **329**(5991): p. 538-541.
35. Nakayama, K.H., et al., *Decellularized rhesus monkey kidney as a three-dimensional scaffold for renal tissue engineering.* 2010. **16**(7): p. 2207-2216.
36. Sokocevic, D., et al., *The effect of age and emphysematous and fibrotic injury on the re-cellularization of de-cellularized lungs.* 2013. **34**(13): p. 3256-3269.
37. Crapo, P.M., T.W. Gilbert, and S.F.J.B. Badylak, *An overview of tissue and whole organ decellularization processes.* 2011. **32**(12): p. 3233-3243.
38. Nagata, S., R. Hanayama, and K.J.C. Kawane, *Autoimmunity and the clearance of dead cells.* 2010. **140**(5): p. 619-630.
39. Zheng, M.H., et al., *Porcine small intestine submucosa (SIS) is not an acellular collagenous matrix and contains porcine DNA: possible implications in human implantation.* 2005. **73**(1): p. 61-67.

40. Badylak, S.F.J.T.A.R.P.B.T.N.A.A.O.P.o.t.A.A.o.A., *Regenerative medicine and developmental biology: the role of the extracellular matrix.* 2005. **287**(1): p. 36-41.
41. Arenas-Herrera, J., et al., *Decellularization for whole organ bioengineering.* 2013. **8**(1): p. 014106.
42. Fu, R.-H., et al., *Decellularization and recellularization technologies in tissue engineering.* 2014. **23**(4-5): p. 621-630.
43. Badylak, S.F., D. Taylor, and K.J.A.r.o.b.e. Uygun, *Whole-organ tissue engineering: decellularization and recellularization of three-dimensional matrix scaffolds.* 2011. **13**: p. 27-53.
44. Berman, B.J.B.h., *3-D printing: The new industrial revolution.* 2012. **55**(2): p. 155-162.
45. Landers, R., et al., *Rapid prototyping of scaffolds derived from thermoreversible hydrogels and tailored for applications in tissue engineering.* 2002. **23**(23): p. 4437-4447.
46. Woodfield, T.B., et al., *Design of porous scaffolds for cartilage tissue engineering using a three-dimensional fiber-deposition technique.* 2004. **25**(18): p. 4149-4161.
47. Kruth, J.-P., et al., *Binding mechanisms in selective laser sintering and selective laser melting.* 2005. **11**(1): p. 26-36.
48. Antonov, E.N., et al., *Three-dimensional bioactive and biodegradable scaffolds fabricated by surface-selective laser sintering.* 2005. **17**(3): p. 327-330.
49. Moroni, L., et al., *Biofabrication: a guide to technology and terminology.* 2018. **36**(4): p. 384-402.
50. Inzana, J.A., et al., *3D printing of composite calcium phosphate and collagen scaffolds for bone regeneration.* 2014. **35**(13): p. 4026-4034.
51. Yang, X., et al., *Collagen-alginate as bioink for three-dimensional (3D) cell printing based cartilage tissue engineering.* 2018. **83**: p. 195-201.
52. Nocera, A.D., et al., *Development of 3D printed fibrillar collagen scaffold for tissue engineering.* 2018. **20**(2): p. 26.
53. Cui, X. and T.J.B. Boland, *Human microvasculature fabrication using thermal inkjet printing technology.* 2009. **30**(31): p. 6221-6227.
54. Xu, T., et al., *Viability and electrophysiology of neural cell structures generated by the inkjet printing method.* 2006. **27**(19): p. 3580-3588.
55. Yanez, M., et al., *In vivo assessment of printed microvasculature in a bilayer skin graft to treat full-thickness wounds.* 2015. **21**(1-2): p. 224-233.
56. Highley, C.B., C.B. Rodell, and J.A.J.A.M. Burdick, *Direct 3D printing of shear-thinning hydrogels into self-healing hydrogels.* 2015. **27**(34): p. 5075-5079.
57. Hinton, T.J., et al., *3D printing PDMS elastomer in a hydrophilic support bath via freeform reversible embedding.* 2016. **2**(10): p. 1781-1786.
58. Luo, G., et al., *Freeform, Reconfigurable Embedded Printing of All-Aqueous 3D Architectures.* 2019. **31**(49): p. 1904631.
59. Parenteau-Bareil, R., R. Gauvin, and F.J.M. Berthod, *Collagen-based biomaterials for tissue engineering applications.* 2010. **3**(3): p. 1863-1887.

60. Maeda, M., et al., *Microstructure and release characteristics of the minipellet, a collagen-based drug delivery system for controlled release of protein drugs.* 1999. **62**(3): p. 313-324.
61. Song, Y., et al., *Engineering of brain-like tissue constructs via 3D Cell-printing technology.* 2020. **12**(3): p. 035016.
62. Iwashita, M., et al., *Brain-stiffness-mimicking tilapia collagen gel promotes the induction of dorsal cortical neurons from human pluripotent stem cells.* 2019. **9**(1): p. 1-17.
63. Puetzer, J.L. and L.J.J.A.b. Bonassar, *High density type I collagen gels for tissue engineering of whole menisci.* 2013. **9**(8): p. 7787-7795.
64. Kim, G., et al., *A cryogenic direct-plotting system for fabrication of 3D collagen scaffolds for tissue engineering.* 2009. **19**(46): p. 8817-8823.
65. Moore, G.L.J.A.b., *Use of azo-dye-bound collagen to measure reaction velocities of proteolytic enzymes.* 1969. **32**(1): p. 122-127.
66. Doyle, A.D.J.B.-p., *Fluorescent labeling of rat-tail collagen for 3D fluorescence imaging.* 2018. **8**(13).
67. Shepherd, D., et al., *The process of EDC-NHS cross-linking of reconstituted collagen fibres increases collagen fibrillar order and alignment.* 2015. **3**(1): p. 014902.